Investigating the speed of sound through different media

Ellie Goodman, Finley Van Barr, Maxwell Milchberg, Jiawen Xiong

Department of Physics, Engineering Physics & Astronomy, Queen's University, Kingston, ON, Canada

2nd April 2023

Abstract

The speed of sound was calculated through different materials by measuring the time taken for a vibrational signal to travel a known distance. The signal was detected at the starting and finishing points using piezoelectric transducers (PZTs). The media investigated include aluminium, acrylic, steel, glass and two samples of wood. The speeds found agreed with the recorded literature values, with the values for the speed through glass, (3300 ±180 ms^{-1}) and steel, (6000 ±370 ms^{-1}) being especially close and within the range of the calculated uncertainty. The young's moduli of each material were also calculated, and it was determined that the wood sample was most likely balsa wood with values of 449 ±5.8 MPa and 790 ±13 MPa.

Introduction and theory

Sound can travel through any medium given there are enough particles to vibrate and pass on energy to their neighbours. For this reason, sound, unlike electromagnetic radiation, cannot travel in a vacuum. Within media, acoustic waves travel at different velocities, dependent on the properties of the material. Two properties we will examine are the density and elasticity of materials.

When a material is dense, its particles are tightly packed together and thus the energy from vibrations can be passed from particle to particle much more quickly than if they were spaced further apart. [1]

Additionally, materials with a high elasticity, represented in solids by the young's modulus, maintain their original shape better. If a force is applied, the particles return to the original positions and are ready to move again more quickly than in a material with a low elasticity. High elasticity materials can therefore vibrate at higher speeds and carry sound faster. [1]

The relationship between these two properties and the speed of sound, v, is given by Equation 1.[2] Here, Y is the young's modulus, and ρ is the density.

$$v = \sqrt{\frac{Y}{\rho}} \tag{1}$$

There are many real-life applications for which it is necessary to know the speed of sound through different media for one, earthquake detection. Earthquakes produce different types of waves, some of which travel along the surface of the Earth whilst others travel through the mantle, as shown in Figure 1. The earthquake can thus be detected at a faraway point much more quickly than the surface, destructive waves actually reach that point. If the

speed at which the waves are travelling at are known, the time the earthquake originated, as well as the time the impact will occur can be accurately estimated. [3]

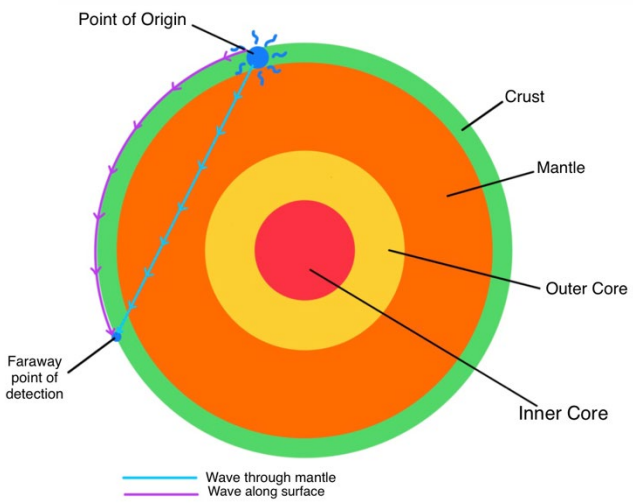

Figure 1: a cross-sectional diagram of the Earth showing how waves travel from an earthquake both along the surface and through the mantle.

The most important and complex piece of apparatus used in this experiment was a piezoelectric transducer (PZT). Understanding of the workings of this device are essential for this study. A PZT contains a crystal which when compressed, generates a voltage. Therefore, when a vibration is detected, a signal is produced and the PZT is acting as a receiver.[4] Conversely, when a voltage is applied, the crystal changes shape, causing a vibration. In this case, the PZT is acting as a transmitter. The same device can be used for two purposed, to transmit or receive vibrational signals. In this experiment, two PZTs were utilised, both acting as receivers.

Also used was a Red Pitaya device which is a multifunction measurement tool with numerous web-based applications.[5] For the purpose of this experiment, the oscilloscope function was used.

Apparatus and Data

A schematic of the experimental set up is given in Figure 2. The triangular structure was built in the workshop and used to suspend rods of different materials. PZTs were in contact with both ends of the rod and both connected to the inputs of the Red Pitaya device. The Red Pitaya was in turn connected to a desktop computer via the Local Area Network using an ethernet cable. It should be noted that an infrared thermometer was kept at the workstation to ensure the temperature remained within a small range of 1°C whilst measurements were being taken.

The PZT on one end of the rod was struck with a hammer, sending a signal directly from that PZT to the Red Pitaya. Meanwhile, a second vibrational signal was propagated through the rod, to the PZT at the other end and again received by the Red Pitaya. As a result, two wavefunctions could be seen on the monitor using the oscilloscope application of the Red Pitaya.

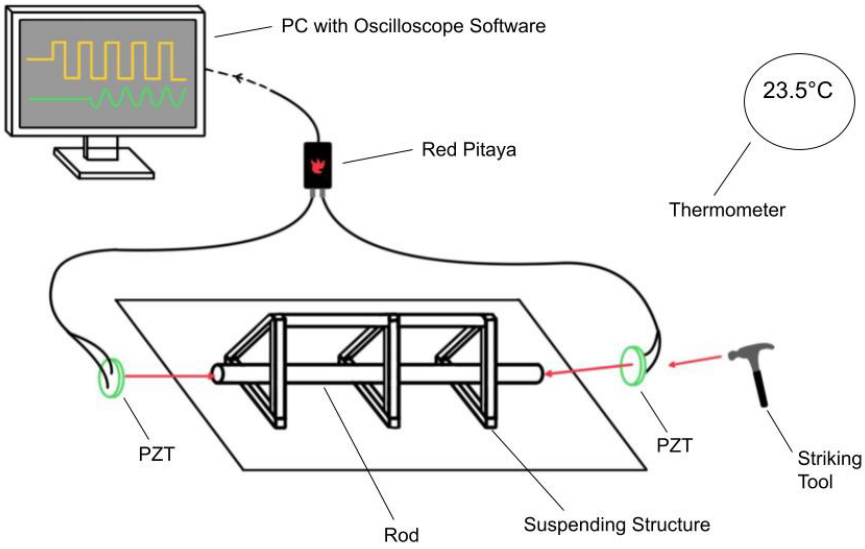

Figure 2: a schematic diagram showing the experimental setup used to measure the time taken for an acoustic wave to travel through a solid rod.

To ensure the maximum vibrational signal was send through the rod, contact with the PZT was minimized. Figure 3 shows how the PZT was held in contact with each end of the rod using a 3-prong clamp and string.

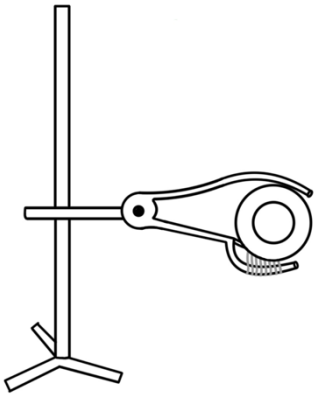

Figure 3: a diagram showing how a 3-prong clamp and string was used to hold the PZT in place with minimal surface contact.

The oscilloscope application has a trigger function which allowed a room noise level to be set. Nothing below this level is recorded and so data was only collected when a signal above this level was detected, in this case, when the rod was struck by the hammer. This allowed minimization of noise as well as better visualization of the instant of detection, which was the only part of the data needed.

The two waveforms were exported as a csv file and a plot was generated using python. From this plot, the time delay between one end of the rod being struck and the signal reaching the other end, was calculated. Knowing the length of the rod, the speed was then calculated using Equation 2.

$$v = \frac{d}{t} \tag{2}$$

This process was repeated three times for rods of aluminium, steel, acrylic, glass, and two wooden rods of different diameters. The plots obtained for each material are shown in Figure 4.

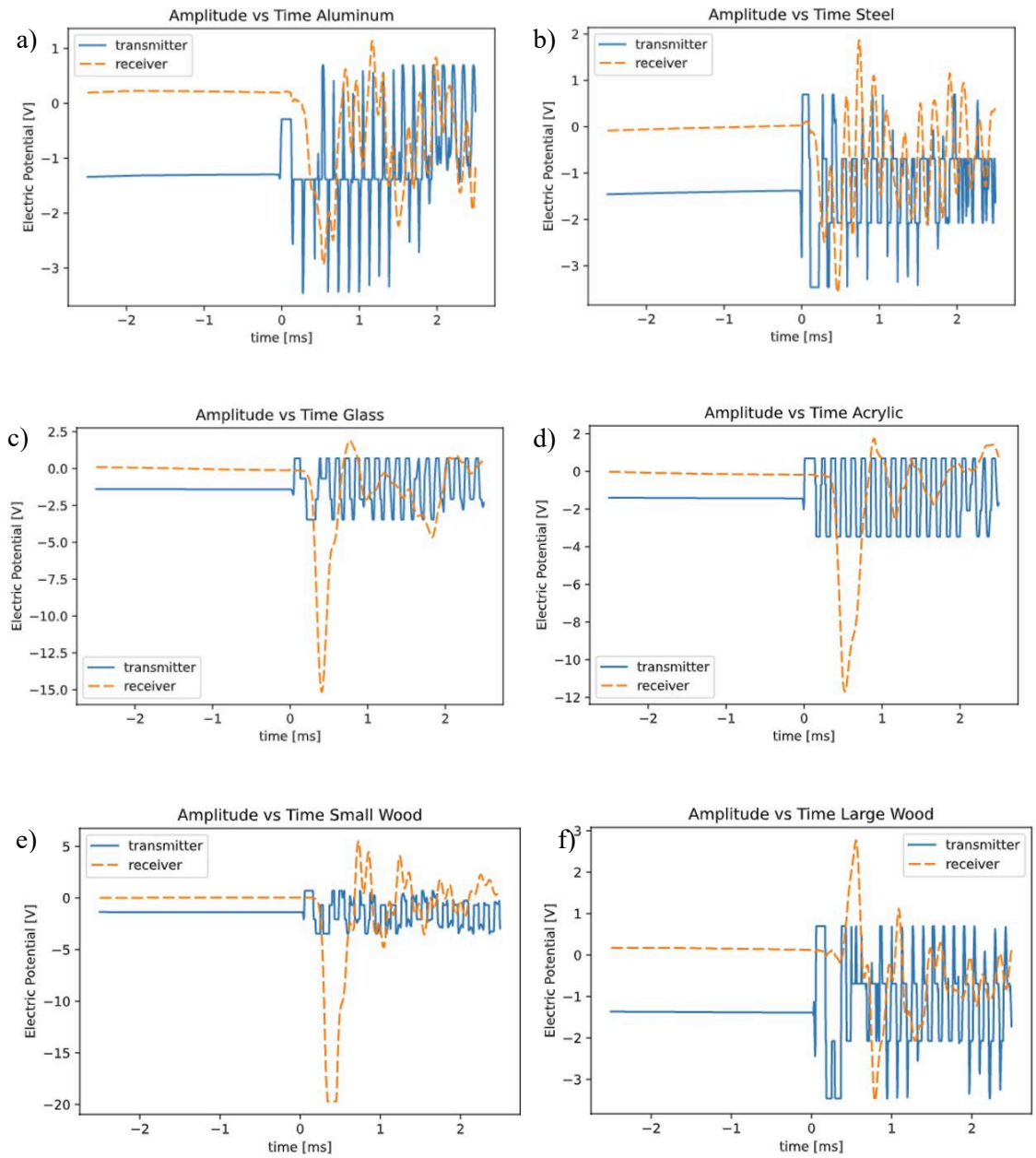

Figure 4: plots generated in python showing the two waveforms detected by the PZTs with data exported from the Red Pitaya oscilloscope function.

It should be noted that initially, the intention was to use a function generator to produce a signal rather than a hammer. However, many technical issues arose, one of which being the conductivity of the metal rods. It is suspected that the electrical signal produced by the PZT was travelling through the rod and being detected before the acoustic signal. This made the

transfer of sound seem almost instantaneous, with the time delay so small it was undetectable by the Red Pitaya. Eventually, it was decided to use the more manual but no less accurate approach of striking with a hammer.

The mass of each rod was measured using an electronic balance and the diameter was measured using callipers. From these measurements, the density of each rod was obtained.

Analysis

Using python, the time at which a signal was first detected was recorded for both inputs. The difference in these times was the time taken for the sound to travel through the rod. These points are better visualized when marked on the plot, as in Figure 5. All the measured and calculated values are given in Table 1 of the Appendix.

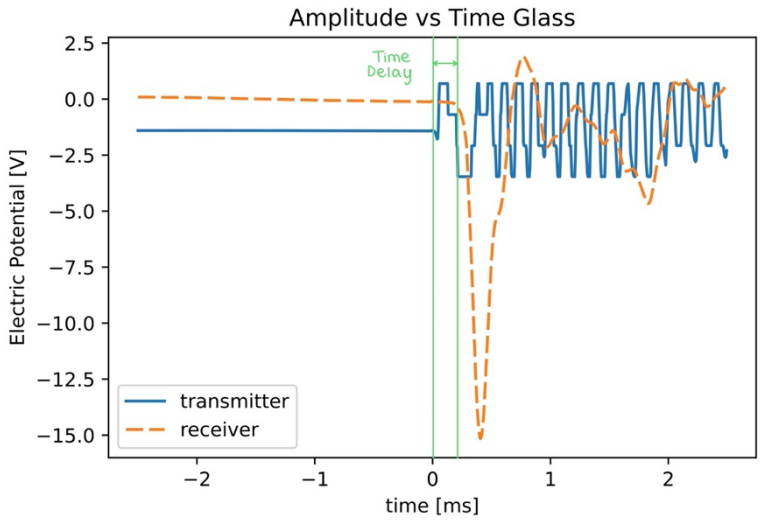

Figure 5: plot of recorded data for glass sample with time delay annotated.

The rods were cut to size in the workshop and given the accuracy of the measuring tools used, the uncertainty in the distance travelled (length of the rod), is ±1mm. The Red Pitaya recorded data every 5μs, therefore, the uncertainty in the time delay is ±5μs due to the sensitivity of the equipment. These uncertainties were propagated using Equation 3 to find the uncertainty in the speed of sound, Δv, for each media where Δt is the uncertainty in time and Δd is the uncertainty in distance.

$$\frac{\Delta v}{v} = \sqrt{\left(\frac{\Delta t}{t}\right)^2 + \left(\frac{\Delta d}{d}\right)^2} \tag{3}$$

Figure 6 shows the speed of sound plotted as a function of density for each material. As expected from Equation 1, there is a square dependence on the density. Errors are shown, calculated from equation 3 although these are very small and not visible for low speeds.

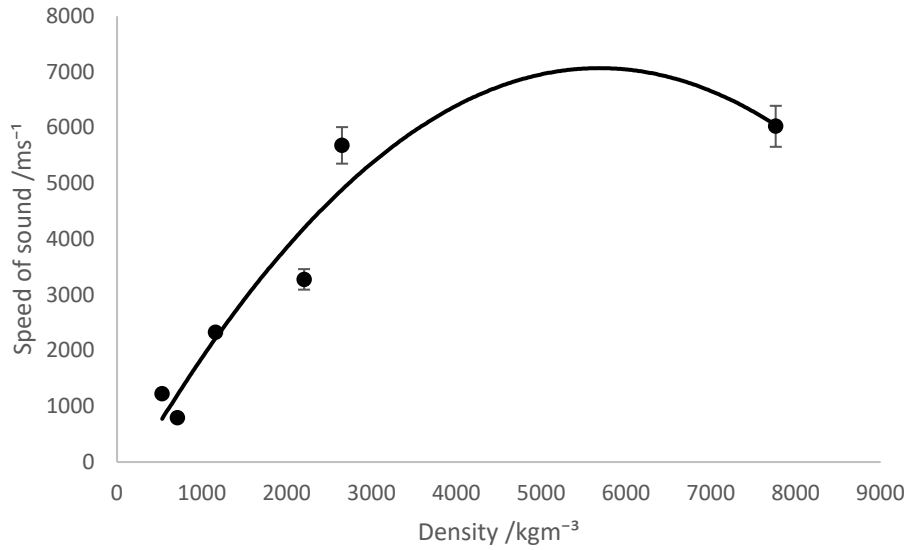

Figure 7: plot showing the speed of sound in ms^{-1} as a function of density in kgm^{-3}.

Similarly, figure 7 shows the speed of sound plotted as a function of the young's moduli. As with the density, a square dependence is seen as expected from Equation 1. This square fit is in better agreement than the density data, suggesting perhaps that the speed of sound has a stronger dependence on the young's modulus than on the density.

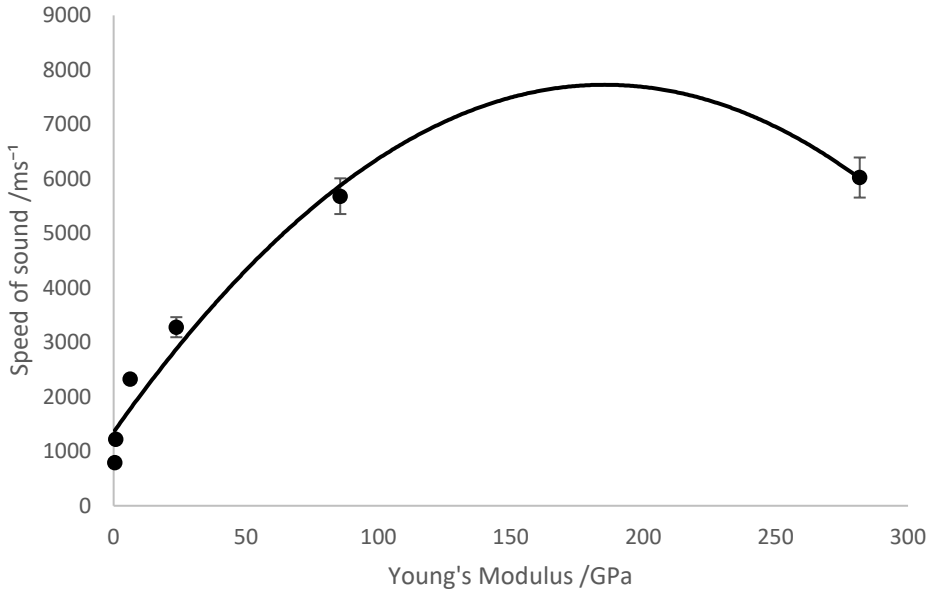

Figure 8: plot showing the speed of sound in ms^{-1} as a function of young's modulus in GPa.

Results and Discussion

Since it is unknown which type of wood the two wooden rods are composed of, it is possible to predict this using their young's moduli. Most woods have young's moduli of over 5000 MPa[6], however the samples we used have values of only (449±5.8) MPa and (790 ±13) MPa.

The uncertainties here were calculated as above described in Equation 3, replacing time and distance with density and speed. It is possible that these are samples of balsa wood, which exhibits an axial Young's modulus of up to 9GPa but a radial Youngs modulus of up to 0.5GPa (increasing with density) [7]. However, this is not certain as wood is anisotropic[8], meaning sound travels at different speeds at different orientations. The speed will be greater along the grain than against the grain. The humidity of the wood[9] may also influence the speed sound travels at.

Perhaps the most encouraging data obtained from this experiment is the comparison of measured speeds to the accepted values in literature, shown in Figure 9. All four of these materials show great similarity to the accepted data, especially glass and steel. Acrylic and aluminium also show calculated speeds close to the accepted values but not inside the uncertainty range. The aluminium sample used in this experiment may not be pure and thus give a different value for the speed of sound. Similarly, acrylic is an entirely synthetic material so it is certain that the composition will be slightly different than that of the sample used in the accepted data.

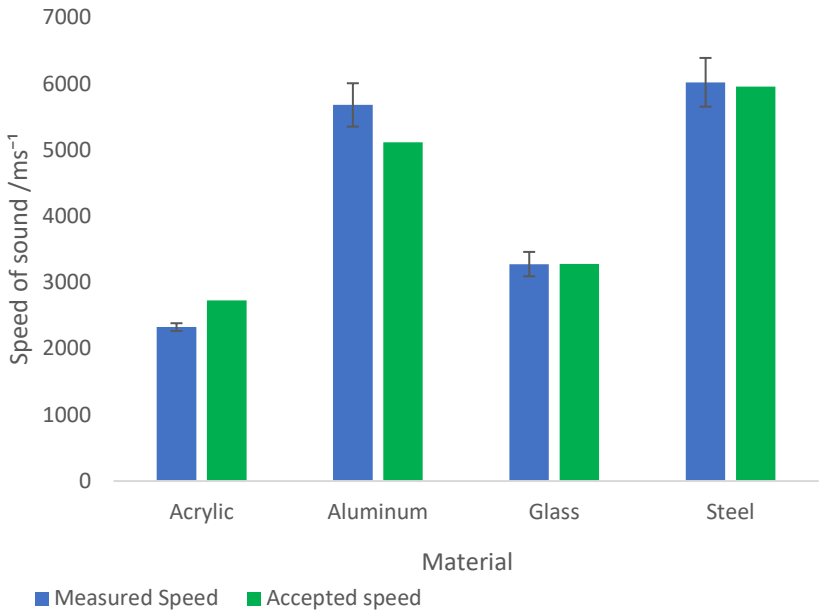

Figure 9: a bar graph showing the comparison of calculated speed values and accepted speed of sound values from the literature.

Conclusion

The speed of sound through acrylic, aluminium, glass, and steel were calculated from the measured time taken to travel a given distance. These calculated values are in strong agreement with values in the literature, however the speeds for acrylic and aluminium lie outside the calculated uncertainty range. There is no way to guarantee that the materials used in this experiment were pure or of similar compositions to those of the recorded values in the literature. This is especially true of glass and acrylic which are synthetic materials with a wide range of possible compositions but also for aluminium and steel which may have differing levels of impurities. For this reasoning, there much disagreement in the

literature for the expected speed of sound through a material, with sources differing often by 1000 ms^{-1}.

It was shown in Figures 7 and 8 that the speed of sound has a square dependency on both the density and the young's modulus of the material, as predicted in Equation 1.

If this experiment was repeated, it may be useful to source samples with exact known compositions. Additionally, smaller PZTs may have a higher sensitivity and give more accurate measurements than those used in this study. Improvements could be made in the density measurements. It would be more accurate to submerge the rod in a measuring cylinder to record the volume rather than calculating from the diameter and length. This would then account for any irregularities in the shape of the rod.

References

1. W. R. Hedrick, "Chapter 1. Properties of Sound Waves," in *Technology for diagnostic sonography*, St. Louis, MO: Elsevier, 2013
2. S. K. Gupta, Engineering Physics; Volume IV; Wave Motion and Sound. Krishna Prakashan Media (P) Ltd., Meerut., 2001.
3. W. R. Matson, Earthquakes; the Sound of Multimodal Waves. [Online]. Morgan & Claypool Publishers, 2016. ISBN: 978-1-6817-4329-5. Available: https://dx.doi.org/10.1088/978-1-6817-4329-5. doi: 10.1088/978-1-6817-4329-5.
4. A. A. Vives (Ed.), Piezoelectric Transducers and Applications. [Online]. Available: https://doi.org/10.1007/978-3-540-77508-9. Springer Berlin, Heidelberg, 2008. Hardcover ISBN: 978-3-540-77507-2. Softcover ISBN: 978-3-642-09624-2. eBook ISBN: 978-3-540-77508-9. Published: May 29, 2008. Edition Number: 2. Number of Pages: XXVI, 532
5. [Online]. Available: https://redpitaya.com. [Accessed: Apr. 01, 2023]
6. Engineering ToolBox, "Wood, Panel and Structural Timber Products - Mechanical Properties," 2011, [Online]. Available: https://www.engineeringtoolbox.com/timber-mechanical-properties-d_1789.html [Accessed: Apr. 02, 2023]
7. M. Borrega and L. J. Gibson, "Mechanics of Balsa (Ochroma Pyramidale) Wood," *Mechanics of Materials,* vol. 84, pp. 75-90, May 2015. [Online]. Available: https://doi.org/10.1016/j.mechmat.2015.01.014.
8. R. L. Ethington and H. C. Hilbrand, "Anisotropy in Wood," Orientation Effects in the Mechanical Behavior of Anisotropic Structural Materials, ASTM STP 405, *Am. Soc. Testing Mats.,* 1966, p. 21-38. [Online]. Available: http://www.astm.org/cgi-bin/doiLink.cgi?STP405-EB.
9. F. F. P. Kollmann and W. A. Côté, Principles of Wood Science and Technology: I Solid Wood. [Online]. Available: https://doi.org/10.1007/978-3-642-87928-9. Springer Berlin, Heidelberg, 1968. Softcover ISBN: 978-3-642-87930-2. eBook ISBN: 978-3-642-87928-9. Published: April 22, 2012.

Appendix

Table 1: Table showing all measured and calculated results.

	Aluminum	Steel	Wood (small)	Wood (large)	Glass	Acrylic
Diameter /cm	2.574 ±0.001	2.554 ±0.001	2.273 ±0.001	4.063 ±0.001	2.540 ±0.001	1.899 ±0.001
Length /cm	50.0 ±0.1	50.0 ±0.1	50.0 ±0.1	50.0 ±0.1	30.9 ±0.1	50.0 ±0.1
Volume	260.182	256.154	202.889	648.266	154.444	141.615
Mass /g	690.01 ±0.01	1988.86 ±0.01	144.74 ±0.01	341.11 ±0.01	340.46 ±0.01	164.39 ±0.01
Density /kgm^{-3}	2562 ±5.5	7760 ±16	713 ±1.5	526 ±1.1	2204 ±7.3	1160 ±2.5
Speed /ms^{-1}	5600 ±330	6000 ±370	790 ±10	1220 ±19	3300 ±180	2330 ±59
Young's moduli /MPa	86000 ±4900	280000 ±17000	449 ±5.8	790 ±13	24000±1300	6200 ±160